August 5, 2011

Down-Type Fourth Generation Quarks in the Lepton plus Jets Decay Channel

Natalee Raymond[1], Katherine Copic[2], John Parsons[2], Evan Wulf[2]

[1]*Macalester College*
[2]*Columbia University*

Abstract

In this paper, I report the search for pair production of the down-type fourth generation quark, b', in a data set of $1.04 fb^{-1}$ integrated luminosity from proton-proton collisions, collected by the ATLAS detector at CERN. Each b' decays promptly to tW in the lepton + jets channel as $b' \rightarrow Wt \rightarrow WWb$. The heavy down-type fourth generation quark decays produce high p_T W bosons which can be identified by reconstructing the di-jet mass.

Contents

1 Introduction

In this analysis, I searched for the existence of the down-type fourth generation quark, b', in the lepton plus jets decay channel. In this channel, the b' quarks are produced in pairs, and the final state contains one leptonically decaying W boson, three hadronically decaying W bosons and two b jets. I searched for the b' in $1.04 fb^{-1}$ of data, obtained from ATLAS, using the number of jets in the events and the number of high p_T $W's$ tagged as discriminating variables.

1.1 LHC

The Large Hadron Collider (LHC) is the world's largest and most powerful particle accelerator. It is located near Geneva on the border between France and Switzerland in a 27 km circular tunnel about 100m underground. CERN, the European Organization for Nuclear Research, is the scientific research center that hosts the Large Hadron Collider. The LHC is designed to collide two counter-rotating beams of protons or heavy ions [1].The proton-proton collisions occur at an energy of 7 TeV per beam. These beams are guided inside the ring by strong magnetic fields created by superconducting magnets under ultra-high vacuum. There are six particle detector experiments at the LHC that are used to examine different research questions. These experiments, Figure 1, are ATLAS and CMS which are the two large general-purpose detectors, ALICE and LHCb which are the medium-sized detectors that are geared towards more specific experiments and the remaining two, TOTEM and LHCf are smaller and focus on interaction of the hadrons that are not in a head-on collision.

Figure 1: Aerial view of the LHC and its six experiments along the France-Switzerland border

1.2 ATLAS

ATLAS, **A** **T**oroidal **L**HC Apparatu**S**, is a detector used at the LHC to investigate a wide range of physical phenomena at the fundamental level. It is 148 feet long, 82 feet wide and high and it weighs approximately 7700 tons. Figure 2 shows an overview of the ATLAS Detector. The ATLAS detector consists of four major components: the Inner Tracker which measures the momentum of each charged particle; the Calorimeter which measures the energies carried by the particles; the Muon spectrometer which identifies and measures muons, and the Magnet system that bends charged particles for momentum measurement [6].

1.2.1 Tracking

The tracking chamber records particle tracks made by electrically charged particles as they ionize matter. The inner detector chamber consists of three sections as seen in Figure 3: the Pixel detector is

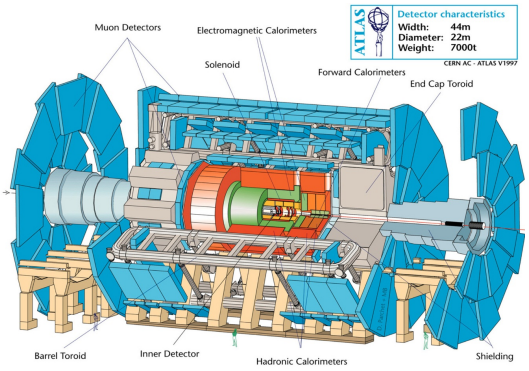

Figure 2: A Horizontal View of the ATLAS Detector

made of 16.4 x 60.8 mm wafers of silicon with 46,080 pixels, 50 x 400 microns each; the Semiconductor tracker (SCT) system, which is designed to provide eight precision measurements per track in the intermediate radial range; and the outer tracker is the Transition Radiation Tracker, a combined straw tracker and transition radiation detector [6].

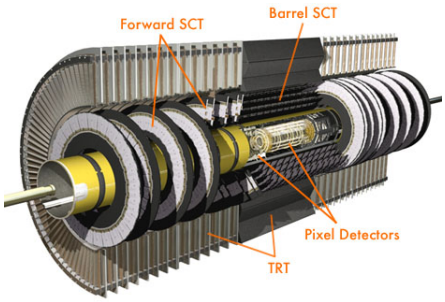

Figure 3: Overview of the ATLAS Tracking System

1.2.2 Calorimeters

The calorimeter stops the electromagnetic and hadronic particles and measures their energies whether they are charged or neutral.The particle goes through the electromagnetic calorimeter and first interacts with a denser material made up of lead metal plates which causes it to shower. The inner section is made up of the Liquid Argon calorimeter and this is the medium that detects the shower of secondary particles. The liquid Argon is under a high electric field and this produces ionization effects for the secondary particles and causes them to drift through the Argon.

The hadronic calorimeter measures hadrons (strongly interacting particles) produced in the interactions. It has two Long Tile Barrels and two Tile Extended Barrels. It is made up of 64x4 submodules and each submodule is composed of alternating tiles of polystyrene and steel separated into 11 tile rows. Steel is the passive medium which means that it only absorbs energy. Polystyrene is the active medium that acts as a scintillating material. Through various processes, molecules and atoms will become excited, and then emit light when they drop to the ground state. The polystyrene registers the photons as calorimeter signals. A systematic view of the calorimeter system can be seen in Figure 4.

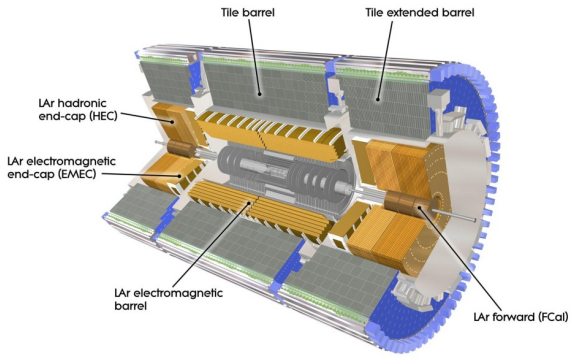

Figure 4: Overview of the ATLAS Calorimeter System

1.2.3 Muon Systems

The Muon chambers are located on the outer layers of a detector because muons are the only charged particles able to travel through meters of dense material as they are affected only by a weak subatomic force, so they don't readily interact with matter.

Figure 5 below shows the tracks of each type of particle throughout the different layers of the ATLAS detector.

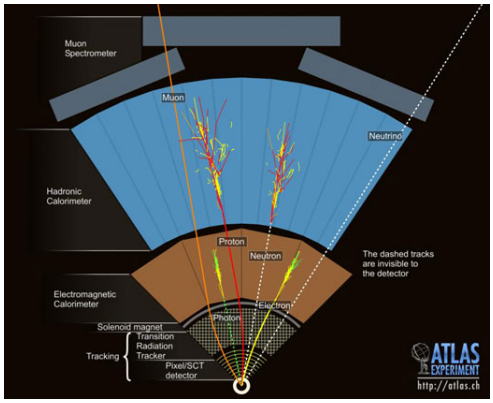

Figure 5: Cross-Sectional View of the ATLAS Detector that illustrates the tracks of each type of elementary particle

1.3 Motivation for Research: The Down-Type Fourth Generation Quark (b-prime)

1.3.1 The Standard Model

The Standard Model (SM) of particle physics is a theory that describes matter as made up of a small number of different types of fundamental particles that interact in a set number of well-defined ways. For the past 40 years, the Standard Model has helped to characterize three of the forces by which the elementary particles interact. These three forces are the Strong, Weak and Electromagnetic forces. Gravity is not in the Standard Model but it is the fourth and weakest fundamental interaction with a relative strength of 1 and an infinite range. The strong nuclear force is the fundamental interaction with the highest relative strength of about 10^{38} times greater than gravity and it is a non-contact force that has a range of about 10^{-15} m. The electromagnetic interaction occurs between charged particles and it

has a relative strength of about 10^{36} times greater than gravity and an infinite range. The weak nuclear force has relative strength of 10^{25}, a range of about $10^{-}18$ m and it is responsible for radioactive decay of subatomic particles. The SM is known for combining three of the fundamental forces within the language of quantum gauge field theories and it combines the electromagnetic and weak interaction into a principle called the electroweak theory.

The Standard Model consists of 12 fermions and 4 bosons/force carriers. The 12 fermions are of spin $-\frac{1}{2}$ and each fermion has its own antiparticle. The fermions can be split into two groups of six: quarks (up, down, top, bottom, strange, charm) and leptons (electron, tau, muon and their respective neutrinos). Pairs of each classification are grouped together to form a generation or families of matter. Both quarks and leptons have three generations that like the periodic table, exhibit similar physical properties (see Figure 6). Leptons do not interact via strong force, however, the electron, tau and muon leptons are electrically charged; hence, they interact via the electromagnetic force. The electron, tau and muon neutrino leptons only interact through the weak force. Because of this they do not carry an electric charge or a color charge. A color charge is another type of charge which is discussed later in Section 1.3.2. The four bosons have integer spins and are force carriers that mediate the strong, electromagnetic and weak interactions. The photon mediates electromagnetic force; gluons mediate the strong force, and the $W^{\pm}$ and Z bosons mediate the weak force.

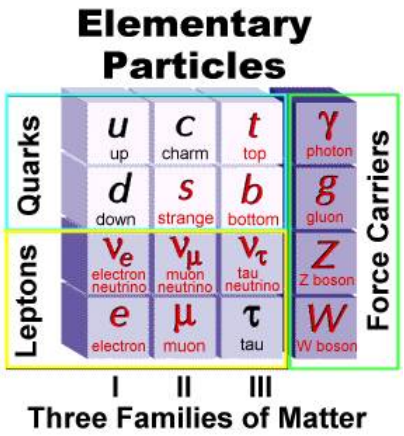

Figure 6: Fundamental particles and Force Carriers according to the Standard Model

1.3.2 Quarks

Quarks experience all four of the fundamental interactions mentioned above. All quarks have mass, electric charge, spin and they do not exist by themselves but instead as composites of color-neutral particles called hadrons. Just as electrically-charged particles interact by exchanging photons in electromagnetic interactions, color charged particles exchange gluons in strong interactions [12].When two quarks are close to one another, they exchange gluons and create a very strong color force field that binds the quarks together [12].There are two basic types of hadron: mesons contain a quark and an anti-quark (of opposite color); baryons contain three quarks (one of each color) [13]. As stated before, the Standard Model accounts for three generations of the fundamental fermions but is agnostic when considering higher generations. The number of generations is not fixed by the theory, as such, it is a natural extension for the SM to include fourth generation quarks. In fact, introducing a fourth generation of quarks may help solve some existing faults in the SM. A fourth generation model could provide a source of particle-antiparticle asymmetry large enough to account for the baryon asymmetry of the universe, and accommodate a heavier Higgs boson (the source of mass generation) that a three-generation model could

not [14].

In this paper, I will report my search for the b-prime, b', down-type fourth generation quark. Because we assume the b' to be chiral with a mass larger than $m_t + m_W$, the top-quark and W boson masses, then the b' will decay dominantly as $b' \to Wt \to WWb$, pair-production. This leads to four W bosons and two b-quarks [17].

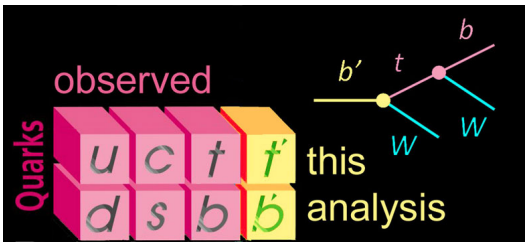

Figure 7: Search for the Fourth Generation Quarks

1.3.3 W-tags

The W boson can decay in two ways: leptonically into a lepton and neutrino; hadronically, into two jets. Missing transverse energy in the events maybe due to neutrinos as they are non-detectable particles. Production and decay of b' pairs (Figure 8) would appear as events with a charged lepton and missing transverse momentum from one leptonically decaying W, and a large number of jets from the two b quarks and the hadronic decays of the other three W bosons [14]. In the lepton + jets decay channel, I look through events with exactly one electron and set out to find two jets that are within a certain closeness of each other. If these jets have an invariant mass consistent with the mass of the W (70-100 GeV), I consider this to be a tagged W.

In the lepton + jets decay channel of $b'\bar{b}'$ we expect to see one lepton, missing transverse energy ($E_{\mathrm{T}}^{\mathrm{miss}}$) from the undetected neutrino, and at least six energetic jets (as shown in Figure 8) [17].

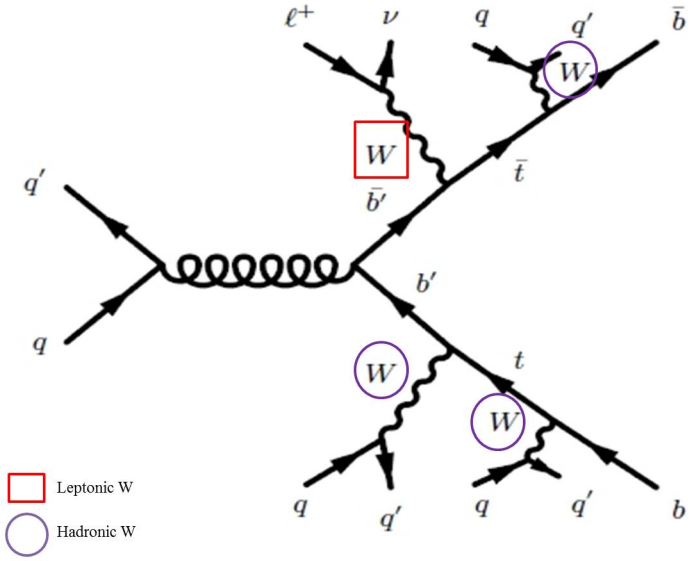

Figure 8: Pair production and decay of b' quarks with decays to $WWbWW\bar{b}$. We select events in which one W decays leptonically and the others decay hadronically.

2 Selection

In order to explain the event selection, we need to define the detector coordinates.

2.1 Definitions of event variables:

- **Detector Coordinates:** The coordinates of the detector are such that the proton beam flows along the z-axis. Figure 9 shows the x-axis and y-axis; ϕ is the azimuthal angle that is in the x-y (transverse) plane and θ is the angle formed in the y-z plane with respect to the proton beam (see Figure 10).

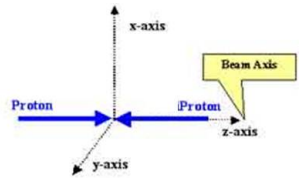

Figure 9: Detector Coordinates

The pseudo-rapidity, η, is defined as:

$$\eta = -\ln(\tan(\tfrac{\theta}{2}))$$

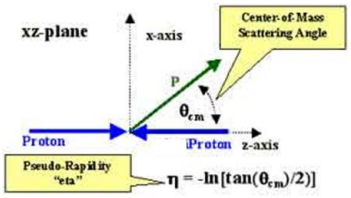

Figure 10: xz-plane

The angular distance, ΔR, labeled d in Figure 11 is the quantity that tells us how close detector objects are from one another:

$$\Delta R = \sqrt{(\Delta\eta)^2 + (\Delta\theta)^2)}$$

ΔR can be thought of as a cone that tells us how close in distance particles are to each other. In Figure 11,there are two jets that are in different cones.

- **Transverse Momentum** (p_T): The momentum measured in the transverse plane:

$$p_T^2 = p_x^2 + p_y^2$$

- **Invariant Mass** (m_T): This is characteristic of the total energy and momentum of a particle that is the same in all frames of reference.

$$M = \sqrt{(E_1 + E_2)^2 - (\vec{p_1} + \vec{p_2})^2}$$

- **Transverse W Mass** (E_T^W): The mass calculated between two particles in the transverse plane:

$$m_T^2(l, v) = 2E_T^l E_T^v (1 - \cos(\phi_{l,v}))$$

- **Transverse Energy** (E_T): This quantity is used synonymously with transverse momentum for electrons due to their small mass.

- **Missing Transverse Energy** (E_T^{Miss}): This is the transverse energy of the neutrino.

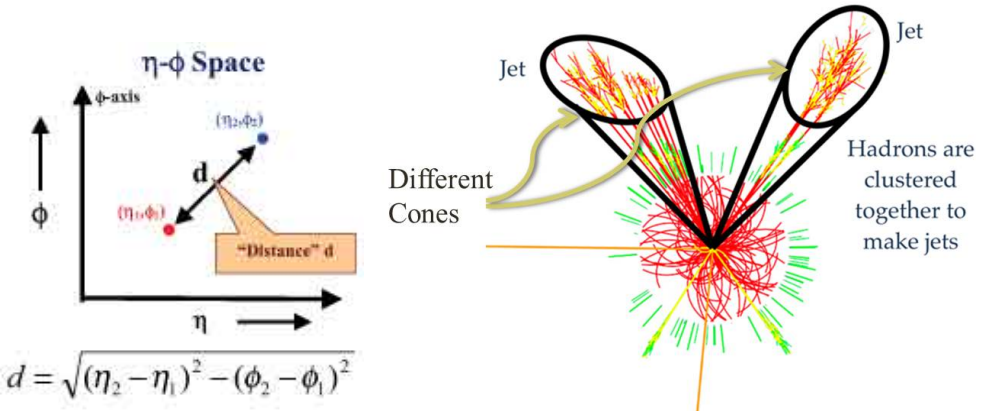

Figure 11: Left: Detector Angular Coordinates; Right: ΔR cone around Jets

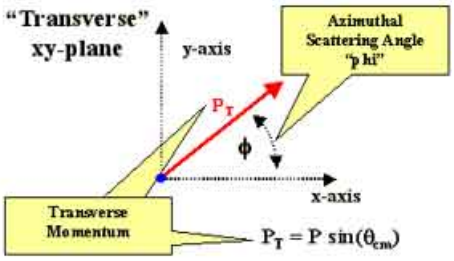

Figure 12: Detector Angular Coordinates

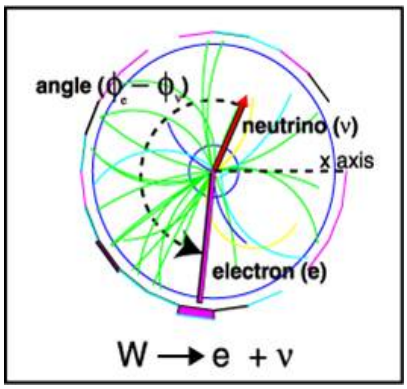

Figure 13: Reconstructing a leptonically decay W boson for transverse W mass

2.2 Object Selection

I applied the object selection defined by the ATLAS Top Group study of the lepton + jets decays of $t\bar{t}$ [17].

- **Electrons:** Electrons were found by a calorimeter-seeded reconstruction algorithm. They were required to satisfy $E_{cluster}/cosh(\eta track) > 25$ GeV in a pseudo rapidity range $|\eta_{cluster}| < 2.47$ but excluding a crack region of $1.37 < |\eta_{cluster}| < 1.52$. Electrons also satisfy calorimeter isolation $I_{cal} < 3.5$ GeV in an $\eta - \phi$ cone of 0.2. I used a corrected isolation provided by the CaloIsoCorrection tool contained in egammaAnalysisUtils-00-02-17, which corrects for pileup and electron p_T leakage. The electron quality requirements match the definition for Tight with a matching track as defined by the electron performance group [23]. Additional electron reconstruction details can be found in [24].

- **Jets:** Jets were reconstructed from topological calorimeter clusters [25] using the $R = 0.4$ anti-kt algorithm [26]. These jets were then calibrated to the hadronic energy scale using p_T jet and η dependent correction factors obtained from simulation [27]. They were required to satisfy $p_T jet > 25$ GeV and $|\eta| < 2.5$. The closest jet to an electron in an $\eta - \phi$ cone of 0.2 is removed, but only electrons that match all other selection requirements are checked. The electron calorimeter cluster η and ϕ were used for this calculation. Additional jet reconstruction details can be found in [28].

- **Muons:** Muons were found with the Muid [29] Combined algorithm, which required that objects detected in the muon spectrometer and reconstructed with the Muid algorithm also have a matched track in the ATLAS inner detector. Muon candidates satisfy $p_T muon > 20$ GeV and $|\eta| < 2.5$. I also required that the muon satisfy calorimeter isolation and tracker isolation requirements (I_{cal} and I_{trk} respectively) of $I_{cal} < 4$ GeV in an $\eta - \phi$ cone of 0.3 and $I_{trk} < 4$ GeV in an $\eta - \phi$ cone of 0.3. Muons must also pass the 'tight' muon requirements as defined by the muon combined performance group [24].

3 Monte Carlo (MC) and Data Samples

3.1 MC Samples

I am searching for the b' quark which has one electron and many jets. Existing Standard Model sources that contain these characteristics are: W+Jets, ttbar, Z+Jets and Diboson (WW, WZ, ZZ) processes. MC samples are also generated for a hypothetical b' with cross sections given according to the theory. The MC backgrounds are scaled to the amount of data taken by dividing the cross section by the number of events in that background and then multiplying the data luminosity ($1 fb^{-1}$). The plot in Figure 14 shows the number of jets in the events with one electron and Missing Energy for the Monte Carlo backgrounds. The $t\bar{t}$ events unlike the rest have more jets in the events because it has to have four or more jets because of the decay from its pair production. The number of events and cross sections for each MC background can be seen in Table 1.

3.2 Data-set

A data-set of $1.04 fb^{-1}$ was used in this analysis, collected with the ATLAS detector from March through to June 2011. In Figure 15, the electron transverse momentum in events with one electron and missing energy is shown. There is some disagreement between the MC and the data and due to QCD

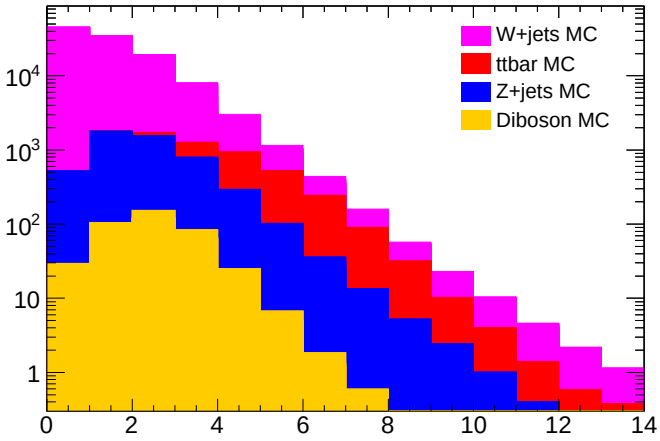

Figure 14: Number of Jets in SM Backgrounds with 1 electron + missing energy

Table 1: Events and Cross-Sections of Monte Carlo Backgrounds.
(NpX) indicates that there are X gluons or quarks produced in addition to the W or Z.

Background	Number of Events	Cross-Sections [pb]
$t\bar{t}$ (Np0)	237284	24.087
$t\bar{t}$ (Np1)	238833	23.814
$t\bar{t}$ (Np2)	146383	14.7315
$t\bar{t}$ (Np3)	93906	9.387
WW	249915	17.02
WZ	249923	5.5424
ZZ	249906	1.2636
W+jets (Np0)	3455037	8305.92
W+jets (Np1)	641361	1565.16
W+jets (Np2)	3768265	435.948
W+jets (Np3)	1009641	121.716
W+jets (Np4)	249869	31.044
W+jets (Np5)	69953	8.4
Z+jets (Np0)	6612265	835.4
Z+jets (Np1)	1333745	167.95
Z+jets (Np2)	404873	50.675
Z+jets (Np3)	109942	13.95
Z+jets (Np4)	29992	3.6
Z+jets (Np5)	8992	1.0375

background which is not modelled with the MC. QCD is a background that produces two hadronic jets in the final states which tend to fake or mimic other particles such as electrons. The cuts made to reduce these backgrounds are the missing transverse energy (MET) and the transverse W mass cuts.

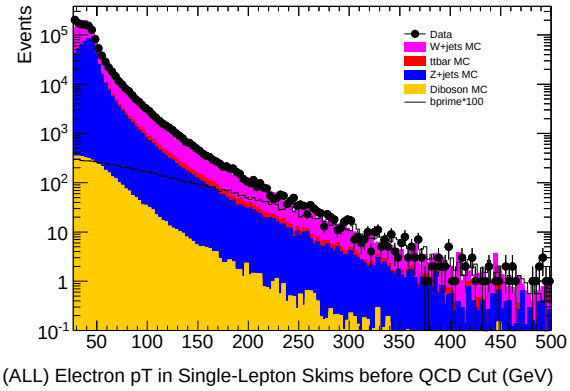

Figure 15: Electron p_T of Single Lepton Skims in GeV. This plot also shows the b' signal (see Section 5). The QCD Cut is discussed in Section 3.3.

3.3 Cuts for Data and MC: E_T^{Miss} (MET) and M_T^W

To reduce QCD backgrounds the following cuts were implemented, which I refer to in most plots as 'QCD Cut':

- $E_{\mathrm{T}}^{\mathrm{miss}} > 35$ GeV and $m_T^W > 25$ GeV

Missing energy is expected to be present given the leptonic decay of the W boson. We discard events with missing transverse energies lower than 35 GeV, because there are very few b' events with low missing energy as there are real neutrinos in the events.

I made a transverse W mass cut of 25 GeV is also applied, to ensure that the events have a leptonically decaying W.

Distributions before and after these cuts for MET, M_T^W, and electron p_T can be seen in Figures 16, 17, 18.

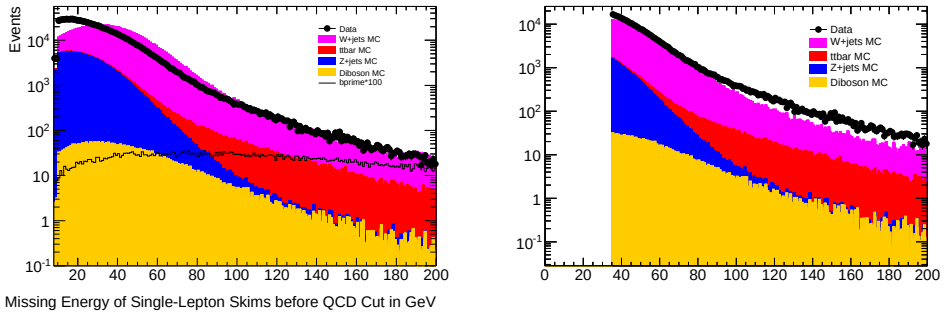

Figure 16: Missing Energy, E_T^{Miss}, of Electrons before and after MET and M_T^W Cuts. At high energies there is a difference between the data and MC that needs to be investigated.

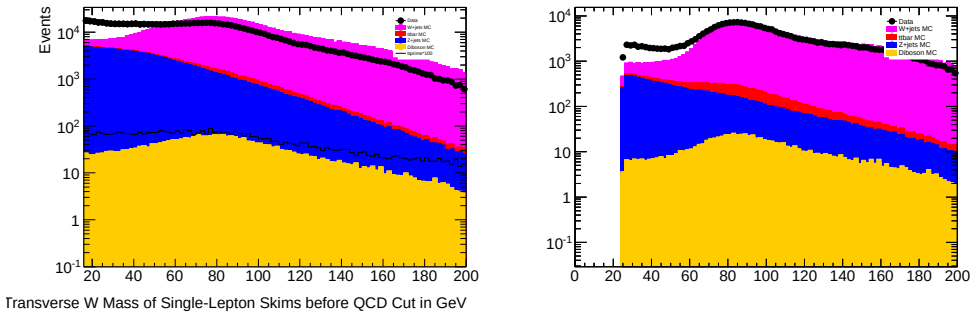

Figure 17: Transverse W Mass, M_T^W, of Electrons before and after MET and M_T^W Cuts. The discrepancy seen at low energies around 25 to 60 GeV just shows the remaining amount of QCD background

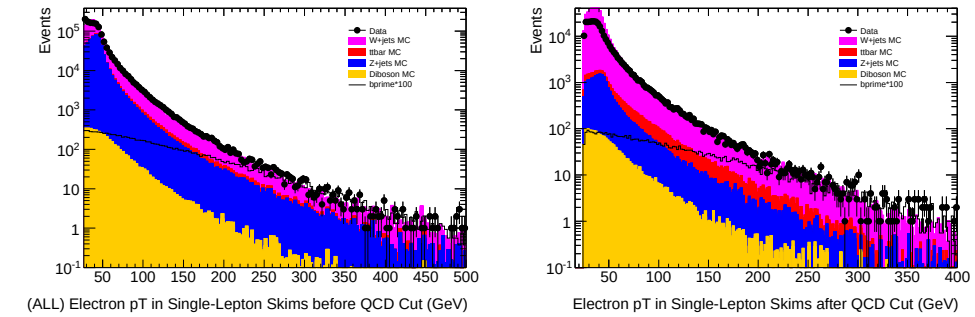

Figure 18: Transverse momentum, p_T, of Electrons before and after MET and M_T^W Cuts. The discrepancy at low p_T is being investigated.

4 Counting W's

To define W-tags, I look for two jets that have $p_T > 25$ GeV, not within $\Delta R = 0.2$ of any electron and are within $\Delta R < 1$ of each other (Figure 19). At high transverse momentum, $W's$ have the jets closer together. If the mass of the jet pairs is within the mass of the W boson (70 to 100 GeV), then it is a W-tag. The Figures 19, 20 show the steps toward making a W-tag.

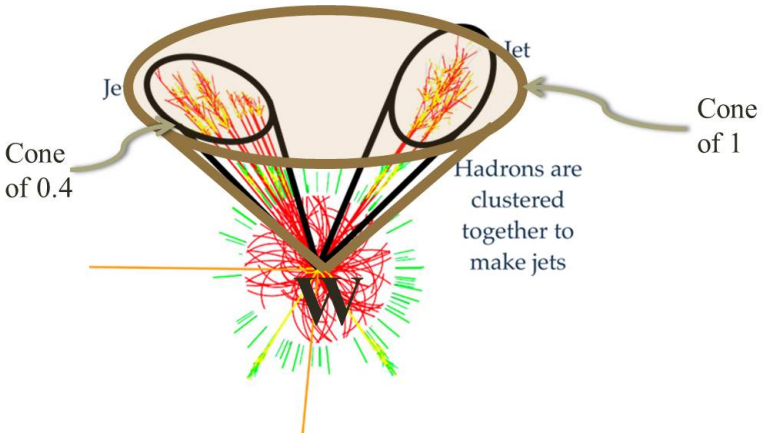

Figure 19: Requirements for W-tag

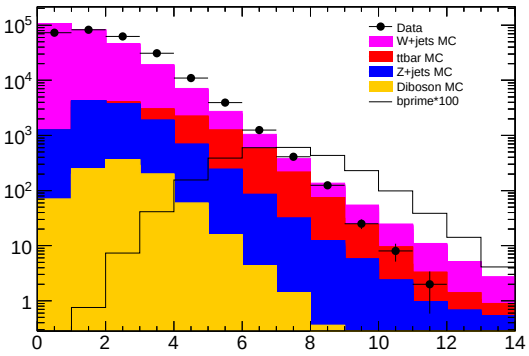

Figure 20: Number of Jets with $p_T > 25$ GeV in events with 1 electron + missing energy before and after MET and M_T^W Cuts.

5 Signal

The signal I used was the 500 GeV mass b'. Figure 23 shows the number of jets in Monte Carlo and Signal events with one electron and missing energy. The b' signal is scaled by a factor of 100 in plots (see Figure 20, 21 for example) otherwise I would not be able to compare it to the other expectations and data.

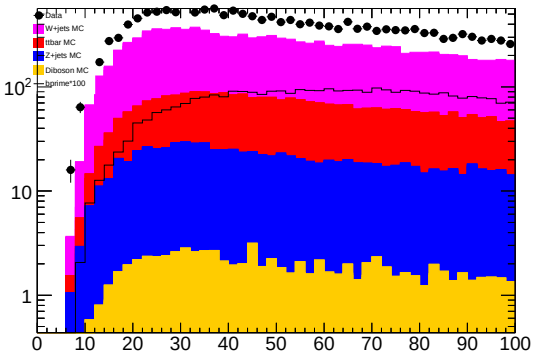

Figure 21: Invariant Mass of Jet Pairs in the Single-Lepton Sample in GeV. This plot shows the invariant mass for every jet pair within $\Delta R < 1$. There can be more than one entry per event.

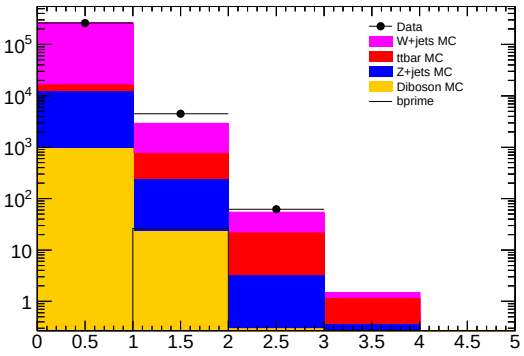

Figure 22: Number of W-tags (N_w in events with 1 lepton + missing energy

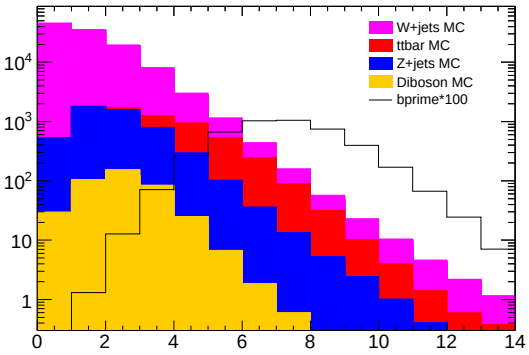

Figure 23: Number of Jets in MC and Signal events with 1 electron + missing energy

5.1 Do we see a Signal in W-tags?

The b' decay is so complicated that we cannot reconstruct the invariant mass. Instead, the number of W-tags is used to help identify which events would be more likely to contain the b' quark. From the W-tags on Figure 21, I made plots of the number of W-tags in events with exactly 6 jets, exactly 7 jets and 8 or more jets. Then, I compared the expected number of b' quarks with those observed in the data. The aim is to see if the data surpasses the expected. This would indicate that something interesting is happening there. In the Figure 24, bin 1 in the $N_{jets} = 6$ plot shows the data surpassing the MC. The number of expected b' quarks for the events with exactly 6 jets and one W-tag is shown by the "bprime" line. Even though the difference in data and Monte Carlo seems to be equal to the amount of b's expected, the possibility of the b' existing there may be ruled out when the uncertainty of the data is taken into consideration.

If there is no difference between the data and the MC, for example bin 3 in the $N_{jets} = 7$ (Figure 24), it is unlikely there will be b' events there because the data agrees well with the SM prediction. If the data are below the MC, then there is very little possibility of b's present in those events. An example of this can be seen in the $N_{jets} = 8$ plot (Figure 24).

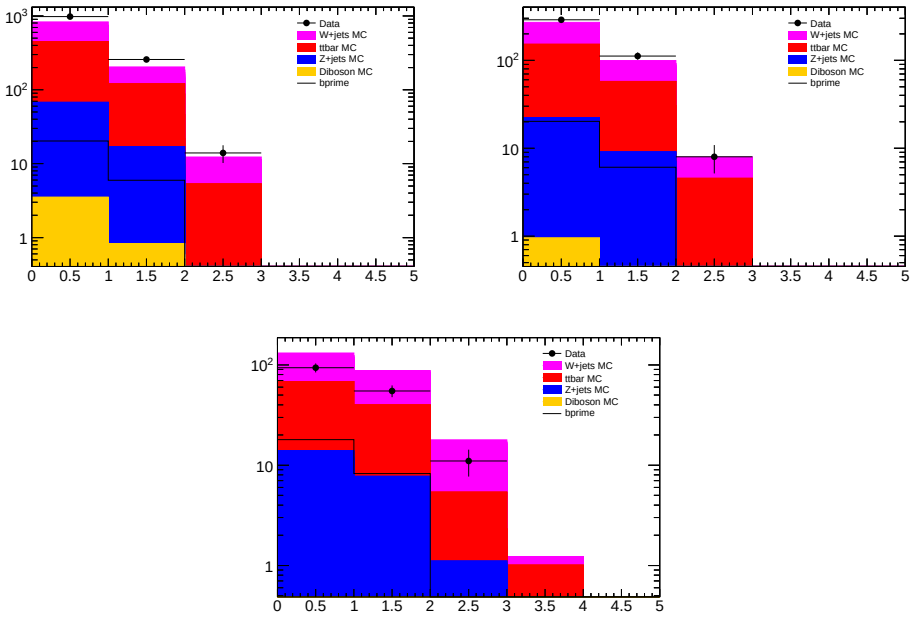

Figure 24: Number of W-tags in events with exactly 6 jets (left), 7 jets (right) and 8 or more jets (bottom) with 1 lepton + missing energy

The existing the limit on the b' in the lepton + jets decay channel, as of the completion of this paper, is > **372 GeV** from CDF. The Limit Plot for ATLAS (Figure 25) is a comparison of the expected limit versus the mass of the b'. The cross-section is related to the number of particles produced. The dashed line is the expected data and the green and yellow sections are respectively 1 and 2 sigma of uncertainty above and below the data. The real data has yet to be plotted on this graph because this is currently an on-going analysis. The blue line represents the theoretical prediction of the cross-section of b' quarks expected to be produced. At the 300 GeV mass b', enough b' quarks should have been produced to be detected. If no excess is observed then this b' mass is then excluded. Different b' masses are excluded until the intersection of the blue and dashed line is reached. Here, the data is insufficient enough to statistically rule out the existence of the b' quark. The same applies for events after the

intersection. The purpose of this plot informs us that if the data agrees well with the expectation, we can get more of a sense of where the b' is excluded.

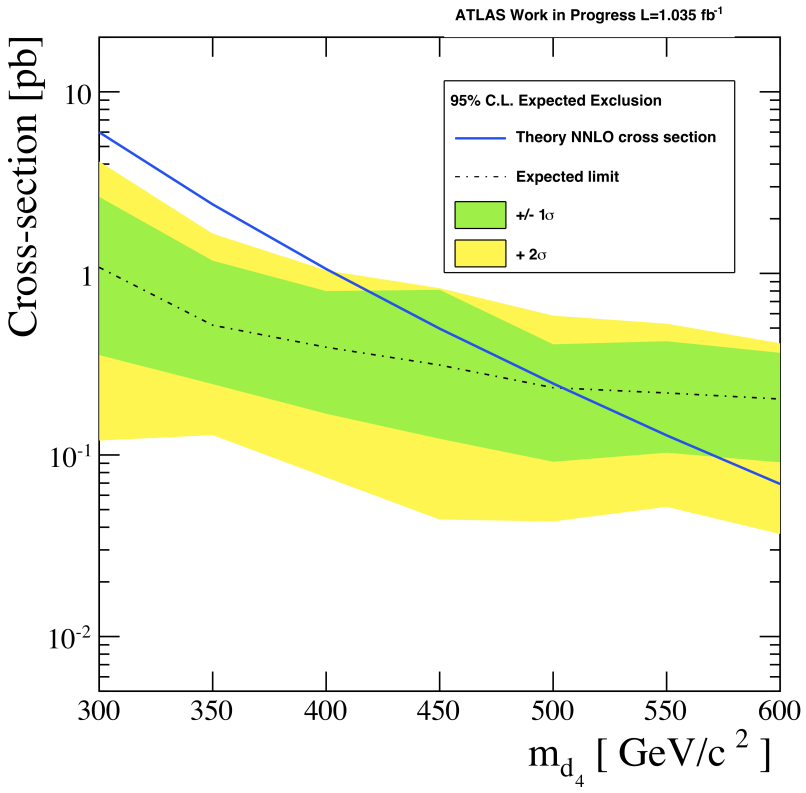

Figure 25: Sensitivity Plot

6 Conclusion

In this analysis, I examined the Lepton + Jets decay Channel for the down-type fourth generation quark, b'. W-tags were made and used for an indication for telling the likelihood of the b' being present in events with one electron + missing energy. As at the completion of this paper the b' has not been found as yet. However, we can expect to exclude up to a 500 GeV b' (see Figure 25), with $1.04 fb^{-1}$ of data.

Appendices

1 Appendix section

To check if my code was working properly, I first ran the program over the Di-lepton Sample. The results are shown below.

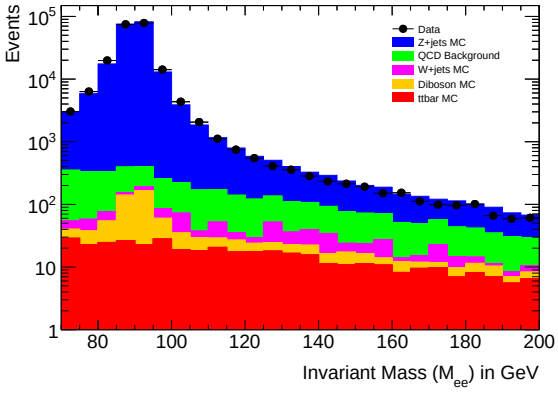

Figure 26: Invariant Mass in the Di-Lepton Sample (Z Peak Normalization)

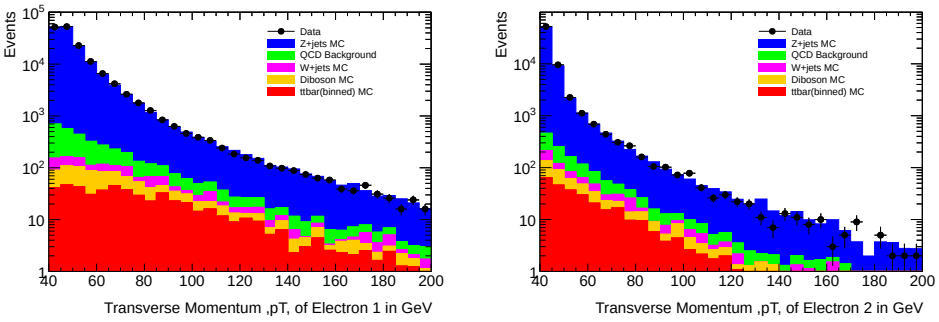

Figure 27: Transverse Momentum of Electron 1 and 2 in the Di-Lepton Sample

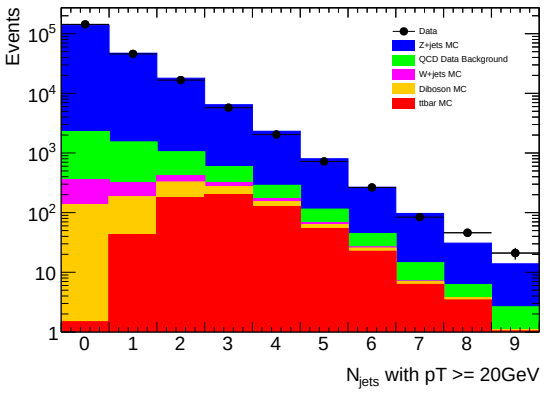

Figure 28: Number of Jets in Events with 2 Electrons of a $p_T \geq 20$ GeV in the Di-Lepton Sample

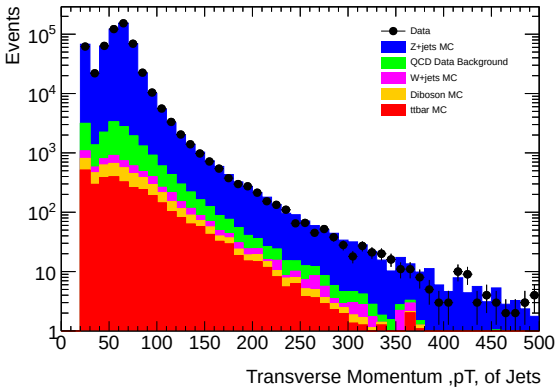

Figure 29: Transverse Momentum of Jets > 20 GeV in the Di-Lepton Sample

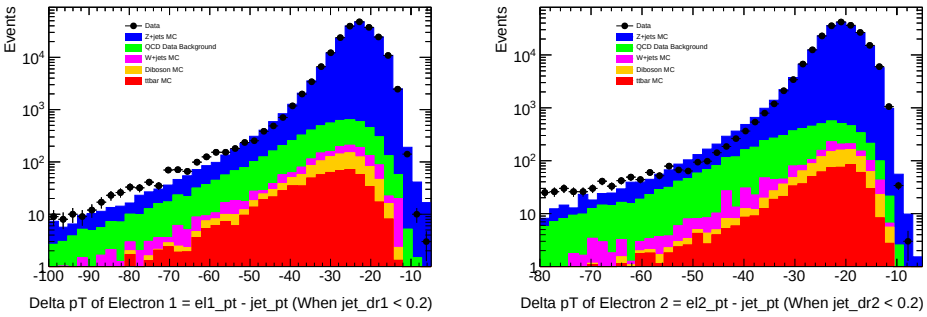

Figure 30: Δp_T for all the jets removed in relation to Electron 1 (Electron p_T - Jet p_T) in the Di-Lepton Sample

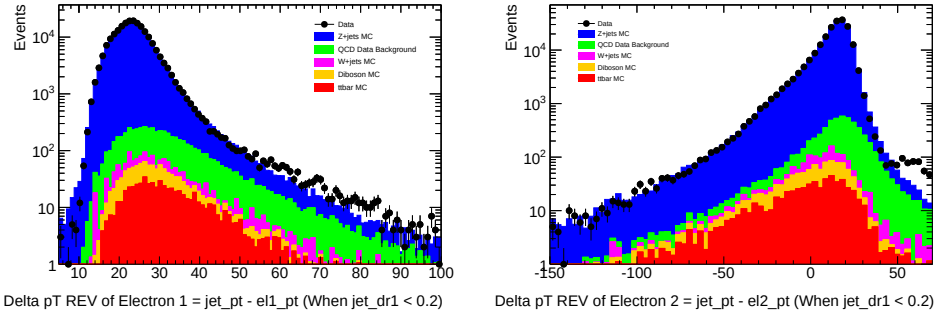

Figure 31: Reverse Δp_T for all the jets removed in relation to Electron 1 (Jet p_T - Electron p_T) in the Di-Lepton Sample

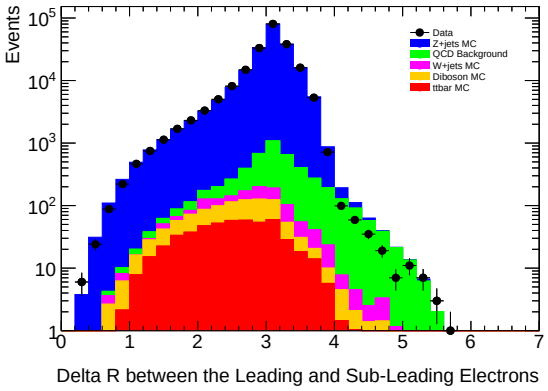

Figure 32: ΔR between Electron 1 and 2 in the Di-Lepton Sample

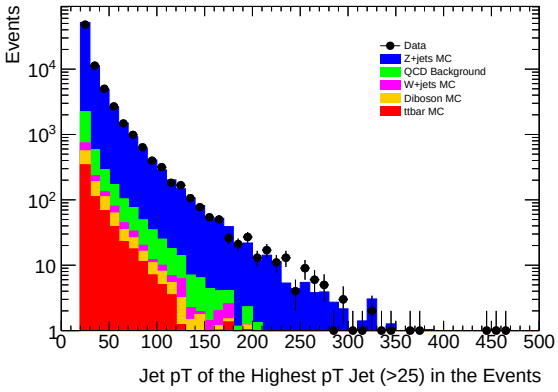

Figure 33: Jet p_T of the Highest p_T Jet (>20) in the Events in the Di-Lepton Sample

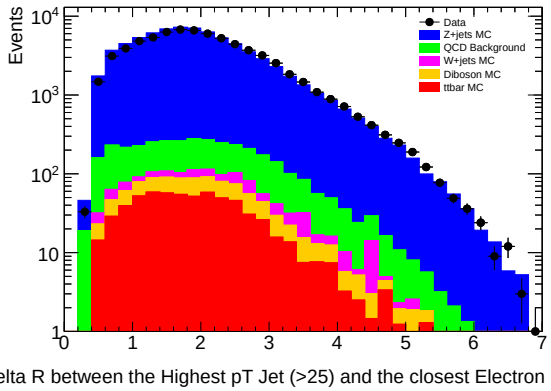

Figure 34: ΔR between the Highest p_T Jet (>20) and the closest Electron in the Di-Lepton Sample

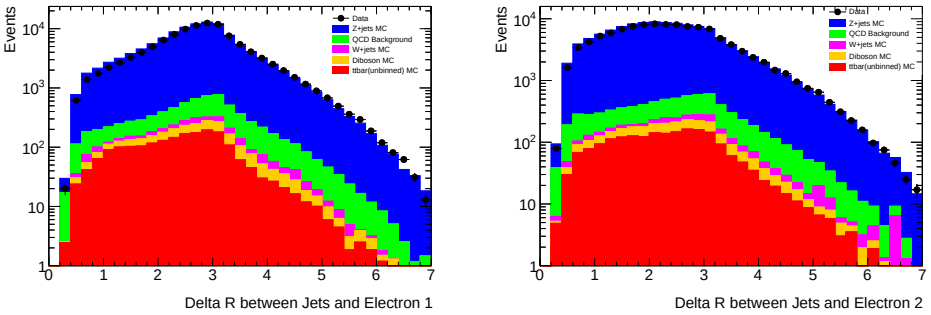

Figure 35: In the Di-Lepton Sample, Left: ΔR between Jets and Electron 1; Right: ΔR between Jets and Electron 2

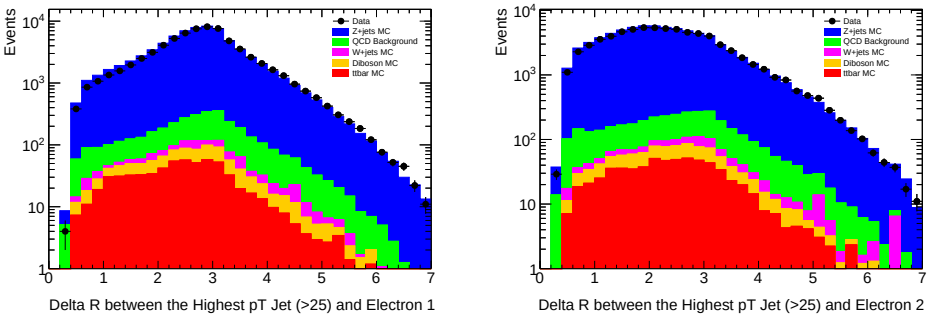

Figure 36: In the Di-Lepton Sample, Left: ΔR between between the Highest p_T Jet (>20) and Electron 1; Right: ΔR between between the Highest pT Jet (>20) and Electron 2

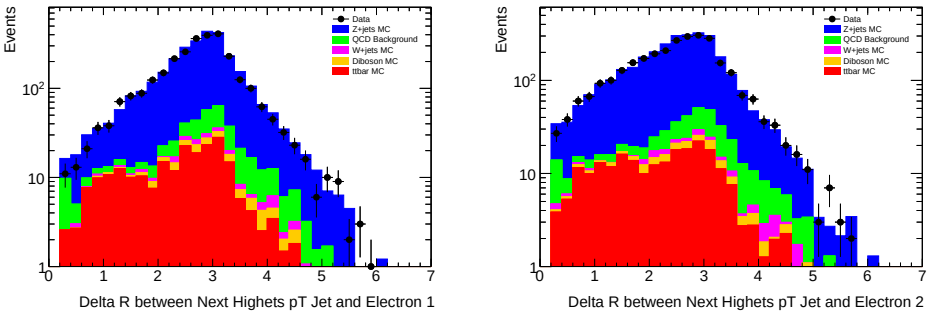

Figure 37: In the Di-Lepton Sample, Left: ΔR between between the Next Highest p_T Jet (>20) and Electron 1; Right: ΔR between between the Next Highest pT Jet (>20) and Electron 2

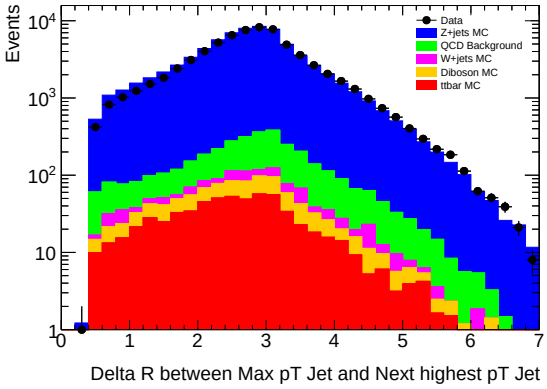

Figure 38: ΔR between the Max p_T Jet and the Next Highest p_T Jet in the Di-Lepton Sample

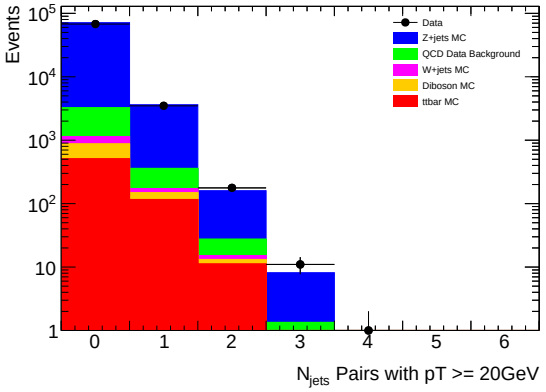

Figure 39: W-tag: Jet pairs within ΔR of 1 of each other that are not close to an Electron in the Di-Lepton Sample

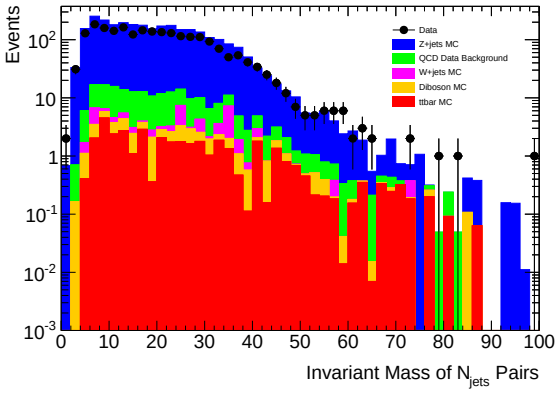

Figure 40: Invariant Mass of Jet Pairs in the Di-Lepton Sample

Bibliography

[1] *LHC Machine Outreach* [http://lhc-machine-outreach.web.cern.ch/lhc-machine-outreach/].

[2] *LHC is Back!!!* [http://faculty.physics.tamu.edu/kamon/research/refColliders/LHC/LHC_is_back.html].

[3] *About the LHC* [http://www.uslhc.us/What_is_the_LHC].

[4] *ATLAS* [http://public.web.cern.ch/public/en/LHC/ATLAS-en.html].

[5] *Syracuse University: Experimental High Energy Physics Educational Outreach* [http://hepoutreach.syr.edu/Index/accelerator_science/accel_overview.html].

[6] *The ATLAS Experiment* [https://twiki.cern.ch/twiki/bin/viewauth/Atlas/WorkBookAtlasExperimen?topic=WorkBookAtlasExperiment].

[7] *The ATLAS Experiment: Mapping the Secrets of the Universe* [http://atlas.ch/inner_detector.html].

[8] *ATLAS Photos* [http://atlas.ch/photos/calorimeters-combined-barrel.html].

[9] *The LHC: a look inside* [http://www.scienceinschool.org/print/651].

[10] M.K. Gillard, P.D.Grannis, F. J. Sciulli, *The Standard Model of Particle Physics* (1998), [].

[11] *Standard Model of Particle Physics* [http://www-sldnt.slac.stanford.edu/alr/standard_model.htm].

[12] *The Particle Adventure* [http://particleadventure.org].

[13] T. Wyatt, *High-energy colliders and the rise of the standard model* (1998), [].

[14] The CDF Collaboration, *Search for heavy bottom-like quarks decaying to an electron or muon and jets in $p\bar{p}$ collisions at $\sqrt{s}$ = 1.96 TeV* (2011), [arXiv:1101.5728].

[15] B. Holdom, W. S. Hou, T. Hurth, M. L. Mangano, S. Sultansoy, G. Unel, *Four Statements about the Fourth Generation* (2009), [arXiv:0904.4698].

[16] A. K. Alok, A. Dighe, D. London, *Constraints on the Four-Generation Quark Mixing Matrix from a Fit to Flavor-Physics Data* (2010), [arXiv:1011.2634 [hep-ph]].

[17] . K. Copic, K. Rao, D. Whiteson, *Search for Down-Type Fourth Generation Quarks in the Lepton plus Jets Channel* (2011), [].

[18] *Searching for a fourth generation* [http://www.fnal.gov/pub/today/archive_2011/today11-03-11.html].

[19] *Pseudo-Rapidity, Azimuthal Angle, and Transverse Momentum* [http://www.phys.ufl.edu/~rfield/cdf/chgjet/z-axis_medium.jpg].

[20] *Pseudo-Rapidity, Azimuthal Angle, and Transverse Momentum* [http://www.phys.ufl.edu/~rfield/cdf/chgjet/eta_def.jpg].

[21] *Pseudo-Rapidity, Azimuthal Angle, and Transverse Momentum* [http://www.phys.ufl.edu/~rfield/cdf/chgjet/etaphi_space.jpg].

[22] *Pseudo-Rapidity, Azimuthal Angle, and Transverse Momentum* [http://www.phys.ufl.edu/~rfield/cdf/chgjet/pt_def.jpg].

[23] The ATLAS Collaboration, *Expected electron performance in the ATLAS experiment* (2010), [ATL-COM-PHYS-2010-990].

[24] The ATLAS Collaboration, *Lepton trigger and identification for the Winter 2011 top quark analyses* (2011), [ATL-COM-PHYS-2011-123].

[25] W. Lampl et al., *Calorimeter Clustering Algorithms : Description and Performance* (2008), [ATL-LARG-PUB-2008-002, ATL-COM-LARG-2008-003].

[26] M. Cacciari, G. P. Salam, G. Soyez, *The Anti-k(t) jet clustering algorithm* (2008), [JHEP **0804**, 063 (2008)] [arXiv:0802.1189 [hep-ph]].

[27] The ATLAS Collaboration, *Measurement of the inclusive jet production cross sections and dijet cross sections in proton-proton collisions at 7 TeV center-of-mass energy with the ATLAS detector at the LHC* (2010), [ATL-COM-PHYS-2010-864].

[28] J.-F. Arguin et al., *Jet selection for top physics* (2010), [ATL-COM-PHYS-2010-835].

[29] D. Fassouliotis et al., *Muon Identification using the MUID package* (2000), [ATL-COM-MUON-2003-003].